Joint Pathology Center
Veterinary Pathology Services

WEDNESDAY SLIDE CONFERENCE 2025-2026

Conference #4 — 17 September 2025

CASE I:

Signalment:
Unknown age, male, black-tailed prairie dog, *Cynomys ludovicianus*

History:
Prairie dog sourced from a zoologic collection. Clinical presentation for acute ptyalism, easily captured, poor vision. Clinical examination noted superficial healing wounds on bilateral forearms, facial scarring with intermittent swellings, incisor malocclusion, elongate buccal aspects of mandibular molars, bilateral tongue ulceration.

Gross Pathology:
External examination of the lungs was normal. On serial sectioning and trimming in representative sections of lung a single small sample of lung tissue was noted as floating low in formalin solution; on examination of one aspect of the cut section the lung was pale tan and consolidated with multifocal pale tan, circular, soft foci (exudate filling bronchi). The total volume of affected lung mass was less than 10%.

Laboratory Results:
Initial Gram, GMS, and acid-fast stains of affected lung tissue did not identify bacterial or fungal microorganisms. Please see comments below for details on follow-up ancillary diagnostics.

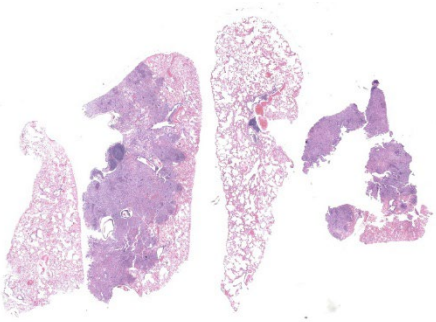

Figure 1-1: Lung, prairie dog. Four sections of lung are submitted for examination, with two sections demonstrating marked consolidation. (HE, 10X)

Microscopic Description:
Lung, multiple sections. Within a single section of lung, approximately 75% of the bronchial, bronchiolar, and alveolar lumina contain overall large numbers of neutrophils, macrophages, large multinucleated cells, cellular debris, homogenous eosinophilic material, fibrillary eosinophilic material, and occasionally scattered erythrocytes. The multinucleated cells are often large and bizarre in appearance, some containing approximately 40 nuclei. The cytoplasm of these multinucleated cells is eosinophilic and variably granular to homogenous. A subset of these multinucleated cells contains few distinct optically clear vacuoles, while others demonstrate phagocytosis of few neutrophils. There is mild vascular congestion throughout, and there are small clusters of lymphocytes cuffing airways multifocally.

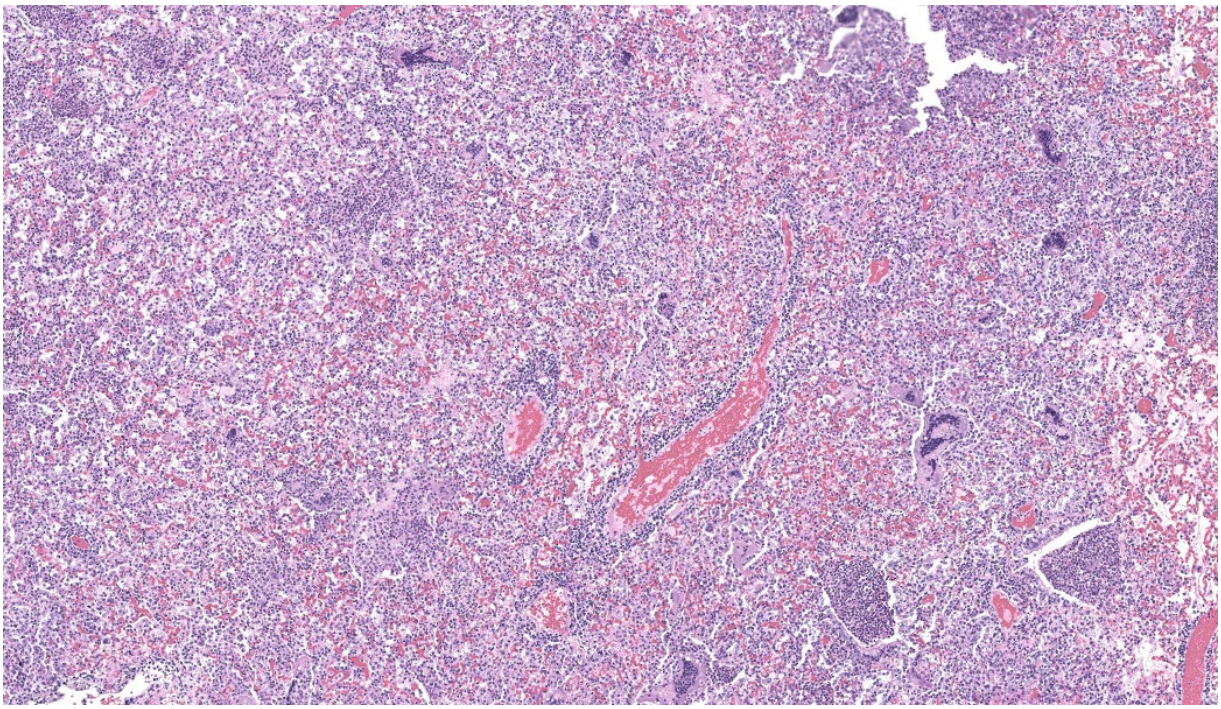

Figure 1-2: Lung, prairie dog. Within affected sections, normal pulmonary architecture is effaced by a dense inflammatory infiltrate expanding alveolar septa and filling alveolar spaces and airways. At this magnification, large multinucleated giant cells and BALT hyperplasia is visible. (HE, 103X)

Contributor's Morphologic Diagnoses:
Pneumonia, bronchoalveolar, suppurative, histiocytic, focal, subacute, severe with intraluminal multinucleated giant cells.

Contributor's Comment:
Initial Gram, GMS, and acid-fast stains of affected lung tissue did not identify bacterial or fungal microorganisms. Viral inclusions were not evident on H&E-stained sections of the affected lung and other tissues evaluated during necropsy evaluation.

Pathologists reviewing the case considered the possibility of multinucleated giant cells versus syncytia. Pulmonary syncytia in mammalian species may be seen with orthopoxviruses, herpesviruses, and respiratory syncytial viruses.[5] Among the orthopoxviruses, monkeypox virus would be a possible differential that must be considered given this species' vulnerability to the virus and the zoonotic potential.[2,7] Necrotizing bronchopneumonia has been reported in prairie dogs with monkeypox viral infection, and histologic descriptions have included syncytia and poorly discernible eosinophilic intracytoplasmic inclusions.[4,6]

Formalin-fixed, paraffin-embedded lung tissue was submitted to the Center for Disease Control and Prevention (CDC) for further evaluation. Immunohistochemical staining for orthopoxviruses was not detected. Additional immunohistochemical stains for canine distemper virus, measles virus, and respiratory syncytial virus were reported negative. PCR testing for human parainfluenza virus (1-4) and respiratory syncytial virus were also reported negative.

Transmission electron microscopy provided ultrastructural evidence of bacteria within giant cells, with no viral particles identified.

The sample was immunoreactive on a polybacterial immunohistochemical assay, but negative for select gram-negative bacteria on a separate immunohistochemical assay. PCR

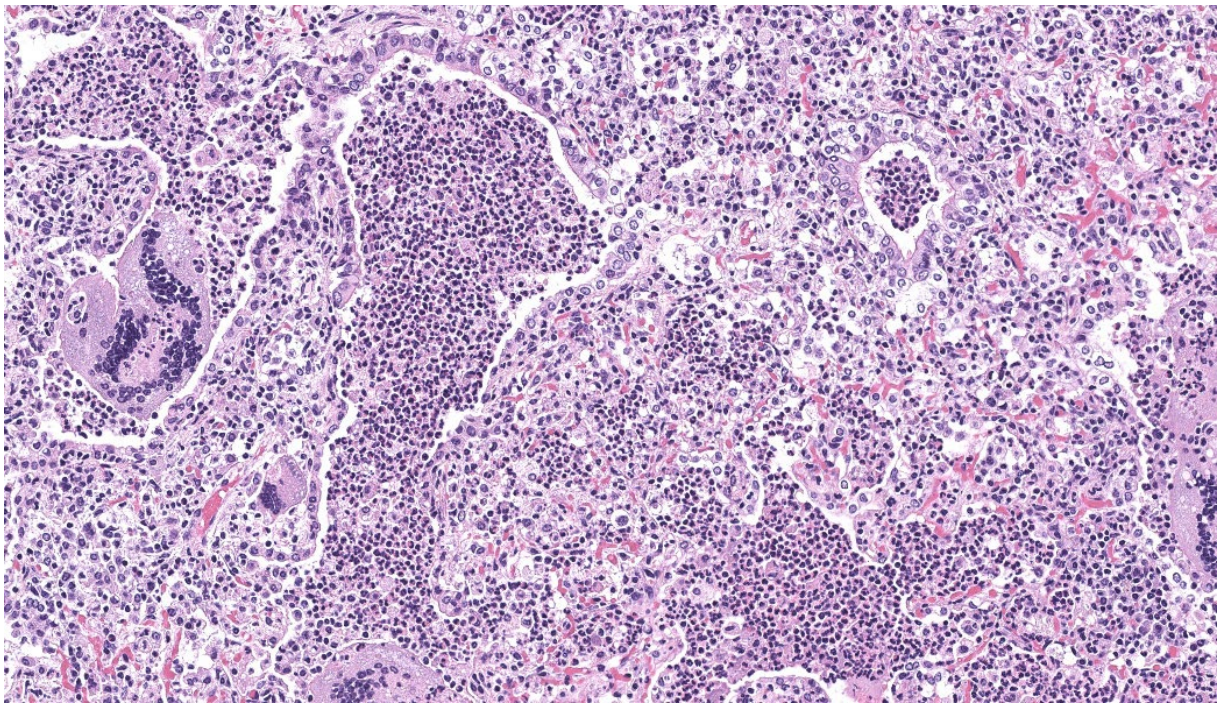

Figure 1-3: Lung, prairie dog. Higher magnification of pulmonary consolidation with expansion of septa by numerous foamy macrophages and fewer neutrophils and scattered multinucleated giant cells with up to twenty nuclei. Airways are filled with similar cells with a higher percentage of neutrophils, and there is multifocal necrosis and loss of airway epithelium. (HE, 285X)

testing for the groEL gene of mycobacteria and *Nocardia* spp. was positive, with subsequent sequencing identifying *Nocardia* spp. PCR testing for gram-negative bacteria specific 16S rRNA gene was positive for Pasteurellaceae. Immunohistochemical staining for *Pasteurella multocida* was negative. PCR testing for gram-positive bacteria specific 16S rRNA gene was indeterminate. Repeat acid fast staining (Fite's stain) identified long filamentous rods within the giant cells.

Contributing Institution:
Arizona Veterinary Diagnostic Laboratory
https://azvdl.arizona.edu

JPC Diagnosis:
Lung: Bronchopneumonia, histiocytic and neutrophilic, chronic, multifocal to coalescing, severe, with numerous multinucleated giant cells.

JPC Comment:
Our fourth conference this year was moderated by the esteemed Dr. Thomas Cecere from Virgina Tech. The JPC team was thrilled to have him back for the second year in a row. This first case provided a great discussion on diagnostic workups and the processes that the pathologist should consider when choosing next steps in a case. Here, the lungs were "chock-a-block" full with histiocytic and neutrophilic inflammation with numerous giant cells that one participant remarked as having "a million nuclei." These were some of the most impressive giant cells that many participants had seen. The bacteria were very difficult to see on the H&E, but the pattern of inflammation and presence of such robust giant cells should clue one into the presence of infectious organisms. As such, next steps should

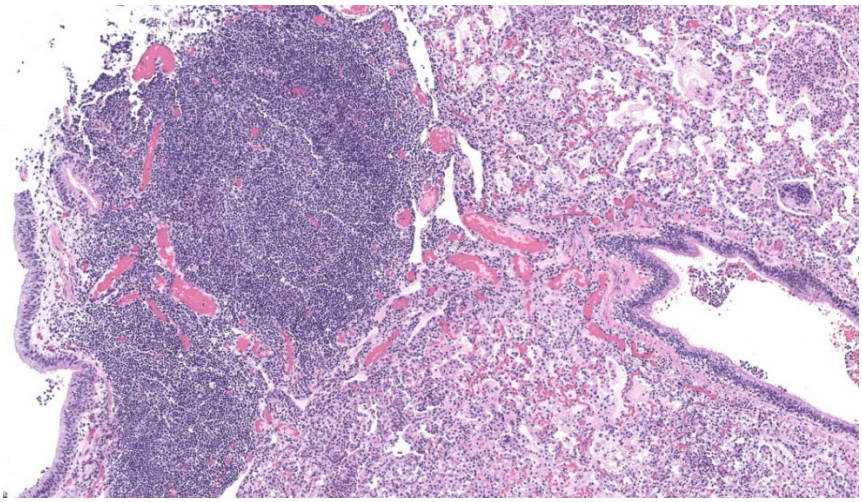

Figure 1-4: Lung, prairie dog. There is significant BALT hyperplasia. (HE, 131X)

include a full gamut of routine infectious organism stains, including gram stains, acid fast stains, and fungal stains (GMS, PAS). Given that these were performed by the contributor, only confirmatory GMS and Fite-Faraco (FF) stains were performed in house, which revealed weakly acid-fast, GMS-positive organisms within multinucleated giant cells. This is consistent with the *Nocardia spp.* that were identified by the contributor. Those "chef's kiss" multinucleated giant cells, though, deserve some recognition here.

The multinucleated giant cell macrophage is a truly remarkable physiologic phenomenon. How they are formed is poorly understood. The current understanding is that macrophages need to be present in chronic inflammation, where they are constantly exposed to pro-inflammatory cytokines, such as IFN-γ, IL-3, IL-4, IL-13, and GM-CSF, as well as pathogen-associated molecular patterns (PAMPs) and other mediators of inflammation.[1] A common setting in which these "ingredients" are found is in fungal infections or when dealing with foreign bodies, both of which can sometimes be too large for inflammatory cells to phagocytose and handle on their own. In this environment, macrophages will be in close association with one another and will begin to express molecules on their cell surface that enable fusion with one another, including dendritic cell-specific transmembrane protein (DC-STAMP; major driver of fusion), β1 and β2 integrins, CD44 (hyaluronic acid receptor), CD47 (integrin-associated protein), macrophage fusion protein receptor (MFPR), fusion regulatory protein (FRP-1, also known as CD98), and P2X7 (an ATP-activated ion channel that results in pore formation).[1]

Now that the involved macrophages have fused together into their version of Infinity Man, they are better equipped with their combined powers to engulf larger threats. One of the mechanisms that multinucleated giant cells have at their disposal to combat pathogens is to produce abundant amounts of nitric

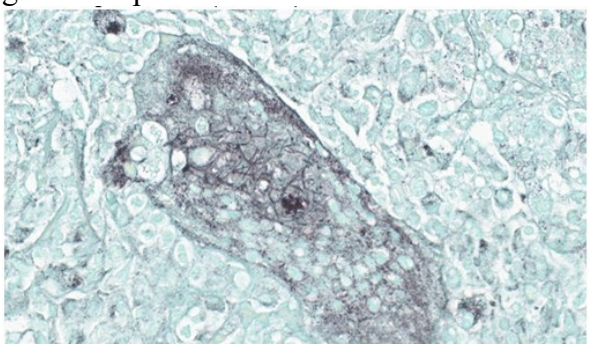

Figure 1-5: Lung, prairie dog. Within the cytoplasm of multinucleated giant cell macrophages, a silver stain demonstrates moderate numbers of haphazardly arranged filamentous bacilli. (GMS, 1189X)

oxide (NO), which is generally microbicidal via induced oxidative stress.[3] However, *Mycobacterium spp.* and *Nocardia spp.* target macrophages as their preferred home within the body and are able to survive intracellularly by preventing fusion of the phagosome and lysosome. Additionally, they produce enzymes to help them combat the damaging effects of NO and other reactive oxygen species produced by macrophages. Multinucleated giant cells are, for all their pathogen-fighting abilities, rather permissive to the persistence of *Mycobacterium spp.* and *Nocardia spp.* within them.[3] With multinucleated giant cells pumping out a ton of NO, other macrophages are additionally induced to fuse and become multinucleated giant cells, which further perpetuates mycobacterial survival and can contribute to the chronic nature of *Mycobacterium spp*. and/or *Nocardia spp*. infections.[3]

References:

1. Ackermann MR. Inflammation and Healing. In: Zachary JF, ed. *Pathologic Basis of Veterinary Disease*. 7th ed. St. Louis, MO: Elsevier; 2022:104-170.
2. Essbauer S, Pfeffer M, Meyer H. Zoonotic poxviruses. Vet Micro. 2010;140:229-236.
3. Gharun K, Senges J, Seidl M, Lösslein A, Kolter J, Lohrmann F, Fliegauf M, Elgizouli M, Alber M, Vavra M, Schachtrup K, Illert AL, Gilleron M, Kirschning CJ, Triantafyllopoulou A, Henneke P. Mycobacteria exploit nitric oxide-induced transformation of macrophages into permissive giant cells. EMBO Rep. 2017;18(12):2144-2159.
4. Guarner J, Johnson BJ, Paddock CD, Shieh WJ, et al. Monkeypox transmission and pathogenesis in prairie dogs. Emerg Inf Dis. 2004;10(3):426-431.
5. Hughes L, Olson VA, Damon IK. Poxviruses. In: Jorgensen JH, ed. Manual of Clinical Micrology. 11th ed. ASM Press; 2015.
6. Langohr IM, Stevenson GW, Thacker HL, Regnery RL. Extensive lesions of monkeypox in a prairie dog (Cynomys sp.). Vet Pathol. 2004;41(6):702-707.
7. Yarto-Jaramillo E. Rodentia. In: Miller RE ed. Fowler's Zoo and Wild Animal Medicine. Vol 8. Saunders; 2015.

CASE II:

Signalment:
12-year-old, female, mixed breed, domestic goat, *Capra aegagrus hircus*

History:
The owners report weight loss and cough for a few weeks. When auscultated, muffled heart sounds were heard on the right side, but no heart sounds were heard on the left side. Crackling sounds were heard in the dorsal lung fields but lungs sounds were absent ventrally. The owners elected for euthanasia and the goat was sent for a postmortem.

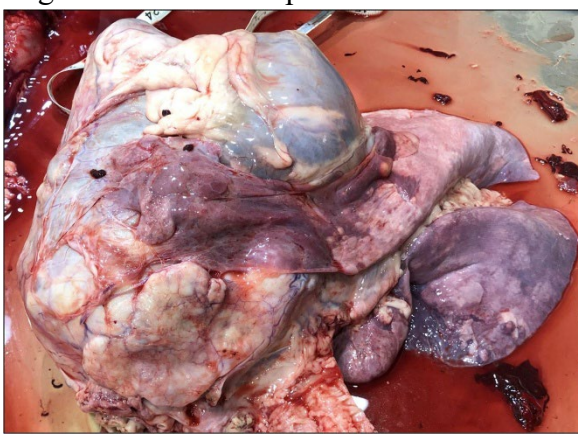

Figure 2-1: Thoracic viscera, goat. There is a large mediastinal mas. Cranioventral lung lobes are multifocally firmly adhered to the outer surface of the mass. Multifocal small nodules are scattered within the lung parenchyma (Photo courtesy of: Atlantic

Gross Pathology:
The goat was thin with small visceral and subcutaneous body fat stores. Moderate clear edema expanded the subcutis and deeper soft tissues along the ventral aspect of the mandibles, the ventral neck and the ventral trunk (dependent edema). Approximately 500 mls of orange-tinged fluid containing a few strands of fibrin was present in both the thoracic and abdominal cavities. Approximately 500 mls of similar fluid also distended the pericardial sac. An approximately 24cm mass expanded the cranial mediastinum and filled the cranioventral thorax, displacing and compressing the lungs caudodorsally. When sectioned, much of the center of this mass was brown, necrotic and composed of many cystic pockets filled with yellow-brown clear fluid intermingled with pale yellow-tan, friable, debris. A thin peripheral layer of relatively intact tissue was generally present just beneath the variably thick layer of dense fibrous tissue which surrounded the mass. Portions of the cranioventral lung lobes were attached by extensive fibrous pleural adhesions to the outer surface of the mass. The pulmonary parenchyma was pale pink, partially collapsed and contained numerous, firm, randomly scattered, nodules ranging in size from 0.7-2.5 cm in greatest diameter. The base of the pulmonary trunk was markedly dilated just proximal to where it entered and passed through the large mediastinal mass. The right ventricular lumen and the right atrium were also markedly dilated. Mediastinal lymph nodes were unremarkable. The liver was diffusely dark red, moderately enlarged and when sectioned had a prominent red brown to tan, reticular (or nutmeg) pattern.

Laboratory Results:
Immunohistochemistry on sections of the mediastinal mass was performed; see microscopic description.

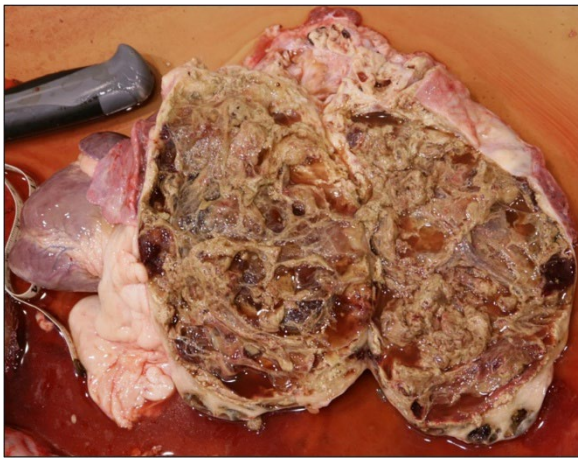

Figure 2-2: Mediastinum, goat. Cut section of the mediastinal mass with a large necrotic center. (Photo courtesy of: Atlantic Veterinary College, University of Prince Edward Island; www.upei.ca/avc).

Microscopic Description:
Much of the center of this mediastinal mass is effaced by extensive areas of necrosis and cystic degeneration. Sections were taken from the remaining thin peripheral rim of intact tissue that is surrounded by a variably thick, dense fibrous capsule. Neoplastic tissue is composed of highly cellular, infiltrates of plump spindled to polygonal cells which are arranged in coalescing trabeculae and sheets and are intermingled with moderate to large numbers of small lymphocytes. These infiltrates multifocally infiltrate the surrounding capsule and are supported by small amounts of fine fibrovascular stroma which often forms dissecting thick bands and thinner septa. Frequently scattered within these infiltrates are small clusters of pale, polygonal, epithelial cells with glassy, keratinized, cytoplasm that are sometimes partially mineralized (Hassall's corpuscles). The interstitium within the mass is also multifocally, mildly to moderately, expanded by pale poorly cellular fine fibrous stroma which often contains variably sized, deposits of basophilic, granular mineral. The majority of neoplastic polygonal to spindloid cells exhibit strong cytoplasmic staining with

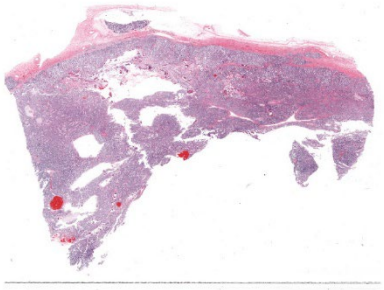

Figure 2-3: Thymus, goat. A section of a mediastinal neoplasm is submitted for examination. There is multifocal capsular invasion. (HE, 10X)

cytokeratin. Most of the small lymphocytes scattered within the mass were CD3 positive.

The masses noted in the lung consist of similar, nodular mixed infiltrates of pale polygonal to spindloid cells intermingled with numerous small lymphocytes. These mixed infiltrates often dilated and fill pulmonary arteries and veins. Frequent scattered small deposits of mineral, foci of lytic and coagulative necrosis are also often scattered within these metastatic nodules.

Contributor's Morphologic Diagnoses:
Malignant thymoma/thymic carcinoma with pulmonary metastasis

Contributor's Comment:
In general, thymic epithelial tumors are considered uncommon tumors in veterinary medicine and have been reported in humans and in a wide range of animals including(but not limited to) dogs, cats, rabbits, cattle, horses and sheep. The exception appears to be in older goats where, although neoplasia is generally uncommon, thymoma was reported as the third most common tumor in a retrospective study involving 100 goats.[5] One report involving a herd of dairy goats (mainly of Saanens or Saanen mixed breeds) found thymomas in 17 of 67 (25.3%) necropsied goats over 2 years of age.[2] Other reports have suggested that pygmy goats may also have a high incidence of thymomas.[3]

In goats, thymomas are often considered benign, slow growing tumors and many are incidental findings at necropsy or slaughter of mature animals. In most species, including goats, thymomas largely reside in the cranial mediastinum. However, due to the anatomy and development of the thymus in ruminants, whereby portions of this large lobulated organ in young animals may extend from the larynx to the cranial aspect of the pericardium, thymomas may form in ventral cervical region, the mediastinum, or involve both locations.[4] When large, as in this case, mediastinal thymomas may result in clinical signs such as respiratory distress and coughing due to compression and displacement of the lung, and trachea. Dependent edema in this goat was attributed to right heart failure caused by compression of the pulmonary trunk as it passed through this large mediastinal mass.

Histologically, thymomas can vary greatly in appearance and in composition. Neoplastic

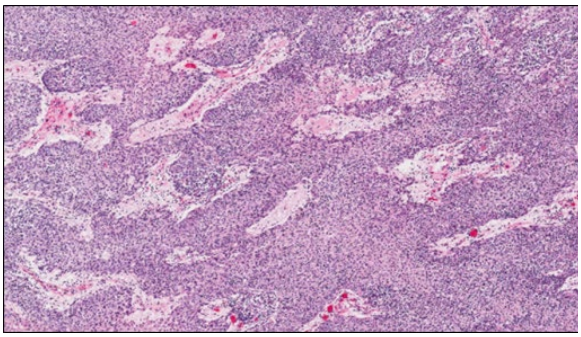

Figure 2-4: Thymus, goat. The neoplasm is composed of coalescing trabeculae and sheets of plump spindled to polygonal tumor cells intermingled with many small lymphocytes. (HE, 4X) (Photo courtesy of: Atlantic Veterinary College, University of Prince Edward Island; www.upei.ca/avc

cells are epithelial and originated from endoderm of the third pharyngeal pouch in the fetus.[2] Tumor cells may appear polygonal and/or spindled, and are accompanied by variable, sometimes large, numbers of mature, non-neoplastic lymphocytes. As in this case, neoplastic cells exhibit cytoplasmic staining with cytokeratins and most of the small lymphocytes present within the tumor are small CD3+ T cells. Thymomas have been subcategorized, based on cellular composition as lymphocyte-predominant, epithelial-predominat, or mixed. A variety of subtypes have also been identified (clear cell, spindle cell, pigmented).[9] A clear association with prognosis and these subtypes has not been identified in veterinary medicine. In human medicine, the 2004 World Health Organization (WHO) classification scheme of thymic epithelial tumors was created to better correlate histologic findings with the clinical behavior of these tumors. This system is also based on the cell morphology of neoplastic epithelial cells and the relative proportion of non-neoplastic lymphocytes present and appears to be applicable to canine thymomas.[10]

Malignant thymomas, or thymic carcinomas, are very rare but have been reported in a variety of species, including goats.[7] As in this case, the previously reported malignant thymoma involved a very large thymoma that had likely been present for a prolonged period and had many small pulmonary metastases. Thoracic lymph nodes were unaffected in the reported case, and in our goat.

A high incidence of paraneoplastic conditions is reported in association with thymomas in both human and veterinary medicine. In dogs, hypercalcemia due to production of PTH-rP is commonly associated with thymomas.[9] Autoimmune paraneoplastic conditions are also commonly associated with thymomas. Most thymomas exhibit varying, and sometimes marked, degrees of lymphopoiesis resulting in the proliferation of polyclonal CD4+ and CD8+ T cells. Normally in humans and animals, naïve T lymphocytes in the thymus interact with thymic epithelial cells which express high levels of MHC I and II molecules. This interaction results in the selection and weeding out of auto-reactive T cells that recognize both MHC molecules and self-antigens.[2] In animals with thymomas, aberrant expression by neoplastic epithelial cells of MHC molecules, autoantigens, and other critical receptors in this selection process, is thought to allow release of CD4+ and CD8+ T cells into systemic circulation which may then react with a wide variety of self-antigens. CD4+ T lymphocytes that recognize self-antigens (such as acetylcholine receptors) stimulate proliferation and differentiation of B lymphocytes with subsequent autoantibody production (resulting in myasthenia gravis and megaesophagus). In some conditions, such as thymoma-associated exfoliative dermatitis (which shares many clinical and histologic

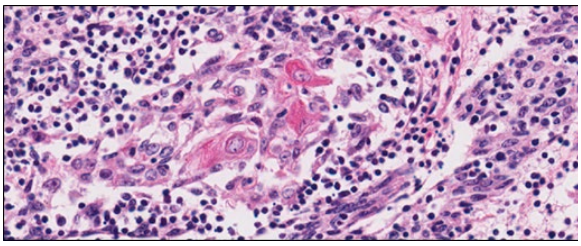

Figure 2-5: Thymus, goat. The neoplasm is composed of coalescing trabeculae and sheets of plump spindled to polygonal tumor cells intermingled with many small lymphocytes. (HE, 4X) (Photo courtesy of: Atlantic Veterinary College, University of Prince Edward I

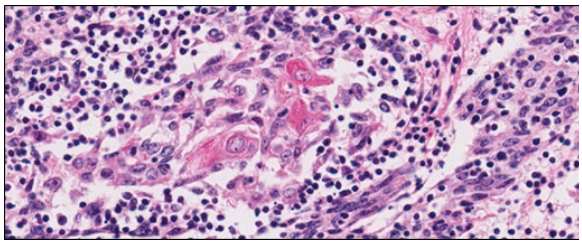

Figure 2-6: Thymus, goat. Small clusters of pale, polygonal, epithelial cells with glassy, often keratinized, cytoplasm (Hassall's corpuscles) are scattered throughout the neoplasm. (HE, 20X) (Photo courtesy of: Atlantic Veterinary College, University of Prince Edward Island; www.upei.ca/avc).

features with erythema multiforme), autoreactive lymphocytes bind directly to keratinocytes and induce apoptosis.[1] A wide variety of additional autoimmune diseases have been reported in animals in association with thymomas including polymyositis, thrombocytopenia, anemia, and granulocytopenia.[9] Paraneoplastic disease in goats with thymomas is extremely rare but megaesophagus and ruminal tympany attributed to esophageal compression by a large mediastinal mass, and thymoma-associated exfoliative dermatitis have both been described in domestic goats.[1,8]

Contributing Institution:
Atlantic Veterinary College, University of Prince Edward Island; www.upei.ca/avc

JPC Diagnosis:
Thymus: Thymoma.

JPC Comment:
The contributor provided an excellent, thorough explanation of thymomas, the paraneoplastic syndromes seen with this neoplasm, and the pathogeneses of how thymomas cause these syndromes. These topics were central to the conference discussion of this case, as well as to the types of questions that were asked of participants about thymomas. As such, the contributor's comment is well-worth a complete read.

Another topic discussed was of the differing types of thymomas classified in human patients and how applicable these are to veterinary medicine. The major thymoma classifications according to the World Health Organization are Types A, A/B, B1, B2, and B3.[6] Type A thymomas are defined by their predominance of spindle-shaped epithelial cells and lack of T-cells.[6] Type A/Bs, also known as "mixed" thymomas, have similar epithelial cell morphology but have an abundance of T-cells throughout.[6] Type B1 has abundant immature T-cells, areas of medullary differentiation, and few epithelial cells.[6] Type B2 is described as having abundant immature T-cells with greater numbers of singular or clustered epithelial cells dispersed throughout the lymphocytes.[6] Lastly, Type B3 has sheets of epithelial cells with rare intercellular bridging and a paucity of T-cells.[6]

Thymoma classification has been discussed in dogs, goats, and sheep predominantly, and there seems to be a shift towards trying to

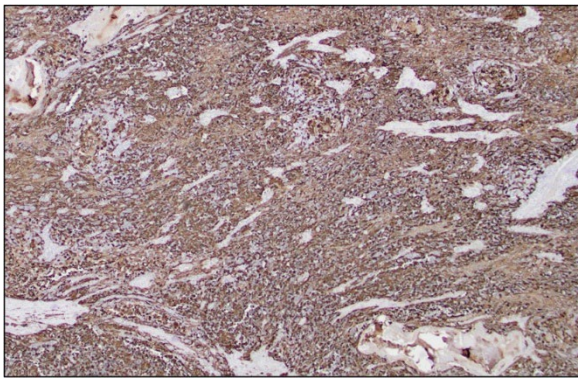

Figure 2-7: Thymus, goat. Neoplastic cells demonstrated strong cytokeratin immunopositivity. (anti-cytokeratin, 40X) (Photo courtesy of: Atlantic Veterinary College, University of Prince Edward Island; www.upei.ca/avc).

align thymoma diagnoses in veterinary species with the classification system that the WHO utilizes for humans. Although it has yet to be fully elucidated whether these classifications are truly comparable in veterinary medi

cine, current literature states that approximately 15% of canine thymomas, as well as the overwhelming majority of thymomas in goats and sheep, are most consistent with Type A/B, although other types have been reported.[10]

References:

1. Byas AD, Applegate TJ, Stuart A, Byers S, Frank CB. Thymoma-associated exfoliative dermatitis in a goat: case report and brief literature review. *J Vet Diagn Invest*, 2019;31(6):905-908.
2. Boes KM, Durham AC. Bone marrow, blood cells and the lymphoid/lymphatic system. In: Zachery JF, ed. Pathologic Basis of Veterinary Disease, 6th ed. St' Louis, Missouri: Elsevier; 2017: 761-764.
3. Hadlow WJ. High Prevalence of thymoma in the dairy goat: report of 17 cases. *Vet Pathol*, 1978;15:153-169.
4. Hill JA, Fubini SL, Hackett RP. Clinical features, treatment, and outcome in goats with thymomas: 13 cases (1990-2014). *JAVMA*; 2017;251(7):829-834.
5. Lohr CV. One hundred two tumors in 100 goats. *Vet Pathol*, 2012; 50(4):668-675.
6. Marx A, Chan JKC, Chalabreysse L, Dacic S, Detterbeck F, French CA, Hornick JL, Inagaki H, Jain D, Lazar AJ, Marino M, Marom EM, Moreira AL, Nicholson AG, Noguchi M, Nonaka D, Papotti MG, Porubsky S, Sholl LM, Tateyama H, Thomas de Montpréville V, Travis WD, Rajan A, Roden AC, Ströbel P. The 2021 WHO Classification of Tumors of the Thymus and Mediastinum: What Is New in Thymic Epithelial, Germ Cell, and Mesenchymal Tumors? *J Thorac Oncol*. 2022;17(2):200-213.
7. Olchowy TWJ, Toal RL, Brenneman KA, Slauson DO, McEntee MF. Metastatic thymoma in a goat. *Can Vet J*, 1996; 37:165-167.
8. Parish SM, Middleton JR, Baldwin TJ. Clinical megaesophagus in a goat with thymoma. *Vet Rec*, 1996; 139:94.
9. Valli VE, Bienzle D, Meuton DJ. Tumors of the Hemolymphatic System. In: Meuton DJ, ed. *Tumors in Domestic Animals*, 5th ed. Ames, Iowa; Wiley Blackwell; 2017: 305-307.
10. Valli VEO, Kiupel M, Bienzle, D, Wood RD. Hematopoietic System. In: Maxie MG, ed. *Jubb, Kennedy, and Palmer's Pathology of Domestic Animals*, 6th ed. St' Louis, Missouri: Elsevier; 2016: Vol 3; 150-158.

CASE III:

Signalment:
Adult, female, Pantaneira, *Ovis aries*, sheep.

History:
On July 24, 2018, the ewe presented with a mild nasal mucohemorrhagic discharge. When rechecked on July 28, 2018 the discharge had become more severe and the ewe was dyspneic and gasping. There was cranium facial asymmetry of the right eye due to exophthalmos. The protrusion of the eyeball resulted in keratitis and corneal ulceration. The ewe was treated with homeopathy with no success. Due to poor prognosis, the ewe was euthanized 34 days after the onset of clinical signs. During July-August 2018, two more cases of the same disease occurred on the premises.

Gross Pathology:
The cadaver denoted poor nutritional status. In the right orbital region, there was a severe increase in periocular volume caused by exophthalmos and resulting in marked cranial asymmetry.

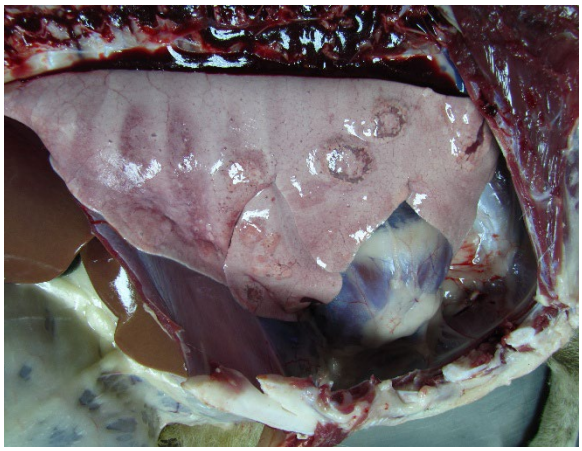

Figure 3-1: Lung, sheep. There are numerous raised nodules, which range up to 2cm and are often surrounded by a red rim scattered throughout the lung. (Photo courtesy of: Universidad Federal de Mato Grosso do Sul, https://www.ufms.br/).

The eyeball was not visible since it was covered by reddish, swollen, ulcerated mucosa. At the cut surface, it was evident that the eyeball had been replaced by a white irregularly outlined mass that was sparsely sprinkled with red spots, with a greyish granular center (caseous material). In the subcutaneous region of the right nasal bone, there was a mass of 2x0.5 cm, the cut surface of which looked similar to that of the ocular mass, but without caseous spots. There was moderate to marked edema throughout the right periocular region.

In the lung, there were several soft, yellowish subpleural nodules of variable sizes (0.5-2cm) and surrounded by a red rim.

The omentum had fair adipose tissue depots, but the serosa of intestines was pale. There were moderate numbers of small hard grey nodules in the serosal aspects of some intestinal loops (calcified nodules of *Oesophagostomum* sp. larvae). The liver was moderately pale, with evidence of the lobular pattern; in the left lobe, there was a firm-to-hard grey nodule interpreted as a calcified hydatid. In both kidneys, irregular pale areas were observed in the natural surface which extended to the cortical region, and in some points reaching the limit of the corticomedullary junction.

On mid-sagittal section of the head, the right side was completely destroyed with loss of nasal conchae which are replaced by a large firm-to-soft, focally friable mass with irregular contours. The mass extended to the pharyngeal region and invaded the cranial cavity, destroying the turbinates and striking the frontal lobe of the brain. After the removal of the cartilage, it was observed that the conchae on the left side were intact but had moderate congestion. After removal of the right hemisphere, an increase in the volume of the olfactory bulb was observed, which was swollen, dark and with a caseous lesion at its junction with the frontal lobe. In the frontal portion of the right cerebral hemisphere, the meninges were thickened, and there was a focal loss of gray matter.

Laboratory Results:

N/A

Figure 3-2: Cerebrum, sheep. A friable mass extends from the nasopharynx through the cribriform plate into the cerebrum. (Photo courtesy of: Universidad Federal de Mato Grosso do Sul, https://www.ufms.br/).

Microscopic Description:
Brain, right frontal lobe: The leptomeninges are focally extensive and moderately expanded by pyogranulomatous exudate. The exudate is formed by nodular to coalescent (mild slide variation) collections of epithelioid macrophages, lesser eosinophils, lymphocytes and plasma cells and few Langhans giant cells. The granulomatous component is admixed with plump fibroblasts, thin bundles of fibrous tissue, and multifocal aggregates of granular, deep basophilic and dense material (mineral). Among the cell debris or in the cytoplasm of the multinucleated cells there are tubularly elongated (when longitudinally sectioned), circular or oval (when transversally sectioned) structures barely stained and hard to visualize in hematoxylin and eosin (HE) stained slide ("negative" images of fungal hyphae). The hyphae are characterized by a body that is hollow or filled with eosinophilic or basophilic granular material and surrounded by varying, but mostly scarce, amounts of strongly eosinophilic, smooth or granular material (Splendore-Hoeppli reaction). The wall of medium-sized arteries in the affected areas is segmentally or cincunferentially expanded by acellular, bright eosinophilic and homogeneous material (fibrinoid necrosis) and occasionally there are hyphae infiltrating the vessel wall or associated with thrombosis in the vessel lumen. There is a focally extensive area of necrosis of liquefaction, swelling of astrocytes and cavitation of nervous tissue, where the parenchyma has been replaced by proliferating microglial cells, many of which already differentiate into foamy macrophages (Gitter cells).

Figure 3-3: Cerebrum and lung, sheep. An inflammatory mass infiltrates the cerebrum at left, and a focally extensive area of consolidation is present in the lung at right. (HE, 10X).

Perivascular cuffs containing up to three layers of lymphocytes are also observed. The organisms stain well by the GMS method as slightly branched hyphae with an irregular diameter of 7-10 μm, associated with foci of necrosis. Occasionally there is a rounded structure of larger diameter (up to approximately 15 μm) at the end of the hyphae.

Lung: There are focal to coalescent areas of consolidation consisting of nodules or sheets of large numbers of epithelioid macrophages and Langhans giant cells admixed with numerous eosinophils and surrounded by fibroblasts and fibrous tissue. The macrophages encircle hyphae similar to that described in the brain that are surrounded by moderate to abundant Splendore-Hoeppli material. Throughout the lung parenchyma there are also small multifocal areas of necrosis containing hyphae. Mineralization is sparsely observed amid necrosis and inflammation. Diffusely, the reminiscent alveolar septa are mildly infiltrated by neutrophils and eosinophils.

Not submitted:

Pyogranulomatous inflammation associated with intralesional hyphae are also observed in

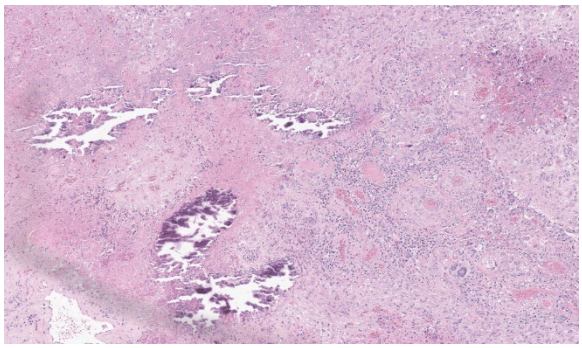

Figure 3-4: Cerebrum, sheep. There is a focally extensive área of coagulative necrosis of the cerebral gray matter (left) with significant pyogranulomatous inflammation with astrocytosis and microgliosis at its periphery. There are scattered aggregates of mineralized debris within the necrotic neuroparenchyma. (HE, 140X).

the nasal conchae, multifocally in the kidneys and expanding eyelids, sclera and periocular tissues.

In the intestinal lamina propria there are small sparsely distributed foci of mineralization, probably mineralized nodules of *Oesophagostomum* sp.

The centrilobular hepatocytes have distended cytoplasm by a sizeable solitary vacuole that pushes the nucleus peripherally (centrilobular lipidosis).

The cytoplasm of the cardiomyocytes is expanded by single, oval structures up to 300 µm in length, filled with elongate banana-like organisms (tachyzoites) consistent with protozoal cysts (*Sarcocystis* sp., most likely *S. bovis*).

Other sections of the brain, spleen, rumen, omasum, and reticulum have no histopathological changes.

Contributor's Morphologic Diagnoses:
Brain, pyogranulomatous meningoencephalitis, focally extensive, with fibrinoid vasculitis and trombi, associated with intralesional fungal hyphae, morphology consistent with *Conidiobolus* sp.

Lung, pyogranulomatous pneumonia, multifocal to coalescent, associated with intralesional fungal hyphae, morphology consistent with *Conidiobolus* sp.

Contributor's Comment:
The lesions presented by this ewe are consistent with nasal zygomycosis of sheep which is a common disease in the semiarid Region of Northeastern and Midwestern Brazil.

The fungi of phylum Zygomycota (zygomycetes) that are of importance as cause of animal disease belong to three orders; Mucorales, Mortierellales, and Entomophtorales.[19] Zygomycetes include widely distributed saprophytes capable of producing opportunistic diseases in animals, and the term zygomycosis is used to describe the illnesses caused by these fungi. Fungi within the order Entomophtorales (entomophthoromycosis) causing animal diseases include (1) *Basidiobolus* spp. reported as a cause of cutaneous granulomas in horses and dogs and (2) *Conidiobolus* spp. reported as responsible for granulomatous inflammation in the subcutaneous tissue of horses; subcutaneous, gastrointestinal and pulmonary granulomas in dogs and nasal granulomas in sheep and horses.[4,5,9,10,12,13,15,16]

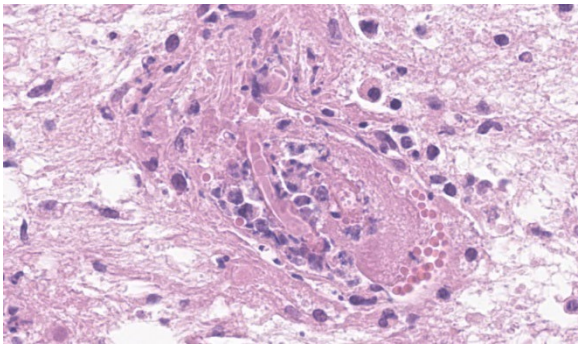

Figure 3-5: Cerebrum, sheep. Thrombosed vessels in the área of necrotic gray matter occasionally contain tangential sections of 6-8um fungal hyphae seen in negative relief. (HE 1400X)

The term zygomycosis is used to describe the diseases caused by fungi mentioned above. In the past, the term phycomycosis was used to refer to infections induced both by zygomycetes and by the fungus-like organism *Pythium insidiosum*, now classified as an Oomycete from the kingdom Chromista.[5,15,16,19] *P. insidiosum* is a well-known cause of eosinophilic subcutaneous and pulmonary granulomas in horses and of similar lesions in several other anatomical sites, including granulomatous rhinitis in sheep and horses.[1,7,14,19,21,24]

In Brazil, granulomatous rhinitis produced by *Conidiobolus* spp. is a common affection of sheep with the highest prevalence in the Northeast and Midwest, but also occurring, although less frequently, in the South.[2,3,6,8,17,18,20,22,23,27,28] The disease can cause significant losses in sheep due to its high lethality rate, that can reach 100%.[2,3]

Infection may occur through spore implantation in the nasal cavity by small traumas as insect bites, as was described in *C. coronatus* infection.[11] Inhalation of fungal conidia from the pasture or possibly inoculation by the sharp-pointed plant parts is the presumed means of infection of the nasal cavity. From there, the microorganism invades adjacent tissues by direct dissemination.[13,27] The extension of the inflammatory reaction to the orbit causes exophthalmia and other injuries of the eye.[1]

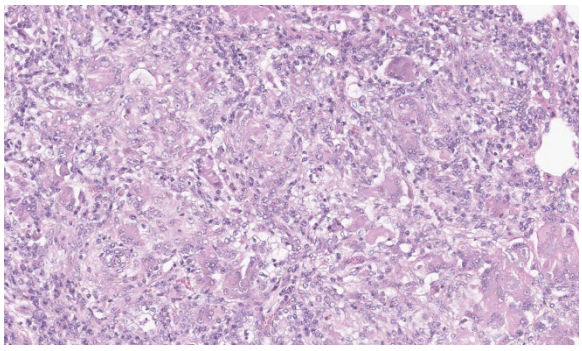

Figure 3-6: Lung, sheep. Within approximately 33% of the section, normal pulmonary parenchyma is effaced by chronic pyogranulomatous inflammation with large numbers of multinucleated foreign body type macrophages. (HE, 381X).

The invasion of the olfactory bulb and frontal lobe of the brain occurs through destruction of the ethmoid bone by the inflammatory process. This has been reported in relation to the rhinopharyngeal form of *Conidiobolus* spp. infection with a prevalence of about 20% to 40 %.[2,13,22,27] In this report the spread also occurred to the lungs, which occurs in this disease with a prevalence of about 15% of the cases, and probably due to aspiration.[8,20,27] The strong effort to breathe may cause fragments of the granulomatous mass to detach and lodge in the lungs, developing new granulomatous foci there.[22] However, dissemination to distant organs such as the kidney, which is reported here, has probably occurred by lymphatic or hematogenous spread. There is evidence for hematogenous dissemination, including mycotic lesions in the vessel walls and invasion of the lumen of vessels associated with thrombosis.

The fungal or fungal-like produced granulomatous rhinitis in sheep occurs in two forms: (1) rhinofacial presentation that affects the nose and the entrance of the nasal fossae and the upper lip,and (2) rhinopharyngeal presentation that affects the turbinates, paranasal sinuses hard, and soft palates and pharynx.[20,21,22,23,27] Over 85% of cases of rhinofacial presentation are caused by *P. insidiosum* and over 90% of the cases of rhinopharyngeal presentation are caused by *Conidiobolus*

spp.[27] In Brazil, *C. lamprauges* and *C. coronatus* have been isolated from these rhinopharyngeal conidiobolomycosis.[3,6,8,22,27,28]

Clinical signs consist of serous nasal discharge that evolves to mucous or mucohemorrhagic; the disease is associated with difficult breathing with stridor, anorexia, and swollen of the anterior or posterior nasal cavity.[4,13]

The tissues of the case reported here were formalin-fixed when they arrived at the laboratory, precluding fungal cultures. Immunohistochemistry and PCR would be the best options to confirm the diagnosis.[27] They were not available to us at the time. So, we had to engage in a diagnostic exercise the allowed us to reach etiology with a reasonably good margin of certainty. A comprehensive review of the lesions affecting the nasal cavity of ruminants in Brazil listed the following five in small ruminants: rhinopharyngeal conidiobolomycosis, rhinofacial pythiosis, aspergillosis, protothecosis and neoplasia (myxoma and enzootic intranasal tumors). After the histopathological examination, only the first two diseases presented a challenge in the differential diagnosis.[18] However, there are significant clinical and pathological differences between rhinopharyngeal conidiobolomycosis and rhinofacial pythiosis that will allow one to reach a final diagnosis. The clinical sign of exophthalmos, due to the presence of retrobulbar granuloma, is a useful indication of rhinopharyngeal zygomycosis.[2,3,4,8,13,17,20,22,27] Although both causal agents may be associated with rhinopharyngeal or rhinofacial presentation of rhinitis in sheep, the location of gross lesions provides a good indicator for the for diagnosis. Disease produced by infection of

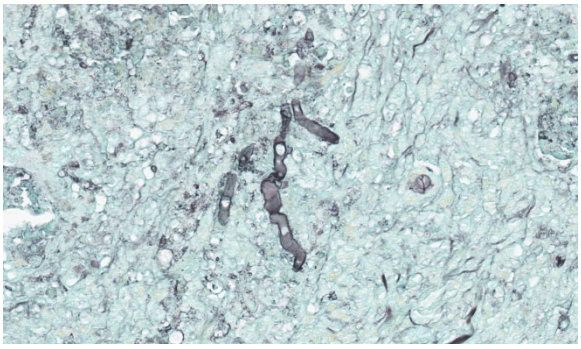

Figure 3-7: Lung, sheep. A GMS stain demonstrates pauciseptate fungal hyphae with non-parallel walls, non-dichotomous branching, and a diameter of 6-8um. (GMS, 674X)

Conidiobolus spp. are almost always rhinopharyngeal and appear as a firm yellow or white mass; pythiosis, almost always located in the rhinofacial region producing a necrotic and friable cellular exudate. Histologically, important morphological differences between the two diseases include the morphology of the two microorganisms. The hyphae in pythiosis have thick walls, almost parallel, and sparsely septate. The hyphae of *Conidiobolus* spp. are thin-walled, non-parallel, and sparsely septate, with ballooning dilations in their extremities.

Enzootic intranasal tumors of ruminants are occasionally diagnosed in cattle and sheep in Brazil, and rhinopharyngitis caused by *Conidiobolus* spp. infection has been mistakenly diagnosed as enzootic intranasal tumor.[18] Although these two conditions have some similar aspects, they can be easily differentiated on histological examination.[26]

Contributing Institution:
Laboratory of Anatomic Pathology, Universidade Federal de Mato Grosso do Sul, https://www.ufms.br/

JPC Diagnoses:

1. Cerebrum:Meningoencephalitis, pyogranulomatous and necrotizing, chronic, focally extensive, severe, with vasculitis, thrombosis, and numerous intravascular and intrahistiocytic fungal hyphae.
2. Lung: Pneumonia, interstitial, pyogranulomatous, chronic, multifocal to coalescing, severe, with vasculitis and intrahistiocytic fungal hyphae.

JPC Comment:

This is an exceptional write-up by the contributor for this conference. Despite not having ancillary diagnostics available to them, they took on this challenge and presented a clear, concise, and well-organized argument for their diagnosis of *Conidiobolus spp.* as the causative agent in this case. The pathologist will not always have additional diagnostics at their disposal in real-world situations, so being able to reason through a case, reach a logical conclusion, and present differentials given the case findings is critical to the profession. Additionally, they provided a succinct overview of the pathogenesis of *Conidiobolus spp*. infections. As far as the case goes, it's almost as if it read the textbook for lesions while providing a diagnostic challenge to conference-goers.

Participants experienced a wide range of emotions during this case presentation due to the difficulty in locating the fungal hyphae on H&E. They are certainly there, but required some squinting to locate and were best found in the sections of cerebrum. Upon revealing the cause, some participants were high-fiving one another out of mutual success while others audibly groaned in dismay.

Discussion focused on indicative features of a zygomycete histologically, which include a broad diameter ranging from 5-15um, non-parallel thin walls, rare septations, asymmetric acute-angle branching, and potentially a terminal bulb. Zygomycetes are typically weakly PAS-positive and more strongly GMS-positive. This correlated nicely with the PAS and GMS stains run in-house. Other differentials mirrored those discussed by the contributor, including oomycetes like *Pythium insidiosum*, which would be PAS-negative and GMS-positive, as well as *Basidiobolus spp.*, another member of the Entomophthoramycota family alongside *Conidiobolus*. However, *Basidiobolus spp.* typically affect the thorax, trunk, limbs, intestinal tract, and, in atypical cases, can cause systemic infection.[28] *Conidiobolus* is far more commonly seen localized to face and nostrils. Using a variety of proteases (including elastase and collagenase), lipases, esterases, and glycoside hydrolases at their disposal, *Conidiobolus spp.* can wreak havoc to the nasal and facial bones and surrounding soft tissues[24]. Ultimately, they may eat through the cribriform plate and enter the brain.[28,29] It's pretty much "game over" at that point.

References:

1. Bianchi MV, Mello LS, De Lorenzo C, et al. Lung lesions of slaughtered horses in southern Brazil. *Pesq Vet Bras*. 2018;38(11):2056-2064.
2. Boabaid FM, Ferreira EV, Arruda LP, et al. Conidiobolomicose em ovinos no Estado de Mato Grosso [Conidiobolomycosis in sheep in the state of Mato Grosso, Brazil]. *Pesq Vet Bras*. 2008;28(1):77-81.

3. Câmara ACL, Soto-Blanco B, Batista JS, Vale AM, Feijó FMC, Olinda RG. Rhinocerebral and rhinopharyngeal conidiobolomycosis in sheep. *Cienc Rural*. 2011;41(5):862-868.
4. Carrigan MJ, Small AC, Perry GH. Ovine nasal zygomycosis caused by *Conidiobolus incongruous*. *Aust Vet J*. 1992;69(10):237-240.
5. Connole MD. Equine phycomycosis. *Aust Vet J*. 1973;49:215-216.
6. de Paula DAJ, Oliveira-Filho JX, Silva MC, et al. Molecular characterization of ovine zygomycosis in central western Brazil. *J Vet Diagn Invest*. 2010;22:274–277.
7. Frade MTS, Diniz PVN, Olinda RG, et al. Pythiosis in dogs in the semiarid region of Northeast Brazil. *Pesq Vet Bras*. 2017;37(5):485-490.
8. Furlan FH, Lucioli J, Veronezi LO, et al. Conidiobolomicose causada por *Conidiobolus lamprauges* em ovinos no Estado de Santa Catarina [Conidiobolomycosis caused by *Conidiobolus lamprauges* in sheep in the state of Santa Catarina, Brazil]. *Pesq Vet Bras*. 2010;30(7):529-532.
9. Greene CE, Brockus CW, Currin MP, Jones CJ. Infection by *Basidiobolus ranarum* in two dogs. *J Am Vet Med Assoc*. 2002;221:528-532.
10. Grooters AM. Pythiosis, lagenidiosis, and zygomicosis in small animals. *Vet Clin North Am Small Anim Pract*. 2003;33:695-720.
11. Gugnani H. Entomophthoromycosis due to *Conidiobolus*. *Eur J Epidemiol*. 1992;8:391-396.
12. Humber RA, Brown CC, Kornegay RW. Equine zygomycosis caused by *Conidiobolus lamprauges*. *J Clin Microbiol*. 1989;27:573-576.
13. Ketterer PJ, Kelly MA, Connole MD, Ajello L. Rhinocerebral and nasal zygomycosis in sheep caused by *Conidiobolus incongruus*. *Aust Vet J*. 1992;69:85-87.
14. Martins TB, Kommers GD, Trost ME, Inkelmann MA, Fighera RA, Schild AL. A comparative study of the histopathology and immunohistochemistry of pythiosis in horses, dogs and cattle. *J Comp Pathol*. 2012;146(2-3):122-131.
15. Miller R, Campbell RSF. The comparative pathology of equine cutaneous phycomycosis. *Vet Pathol*. 1984;21:325-332.
16. Miller R, Pott B. Phycomycosis of the horse caused by *Basidiobolus haptosporus*. *Aust Vet J*. 1980;56:224-227.
17. Pedroso PMO, Dalto AGC, Raymundo DL, et al. Rinite micótica nasofaríngea em um ovino Texel no Rio Grande do Sul [Rhinopharyngeal mycotic rhinitis in a Texel sheep in Rio Grande do Sul]. *Acta Sci Vet*. 2009;37(2):181-185.
18. Portela RA, Riet-Correa F, Garino-Junior F, Dantas AFM, Simões SVD, Silva SMS. Doenças da cavidade nasal em ruminantes no Brasil [Diseases of the nasal cavity of ruminants in Brazil]. *Pesq Vet Bras*. 2010;30(10):844-854.
19. Quinn PJ, Markey BK, Leonard FC, Fitz-Patrick ES, Fanning S, Hartigan PJ. Zygomycetes of veterinary importance. In: *Veterinary Microbiology and Microbial Diseases*. 2nd ed. Oxford, UK: Wiley Blackwell; 2011:466-451.
20. Riet-Correa F, Dantas AFM, Azevedo EO, et al. Outbreaks of rhinofacial and

rhinopharingeal zygomycosis in sheep in Paraíba, northeastern Brazil. *Pesq Vet Bras*. 2008;28(1): 29-35.
21. Santurio JM, Argenta JS, Schwendler SE, et al. Granulomatous rhinitis associated with *Pythium insidiosum* infection in sheep. *Vet Rec*. 2008;163(9):276-277.
22. Silva SMMS, Castro RS, Costa FAL, et al. Conidiobolomycosis in sheep in Brazil. *Vet Pathol*. 2007a;44:314-319.
23. Silva SMMS, Castro SC, Costa FAL, et al. Epidemiologia e sinais clínicos da conidiobolomicose em ovinos no Estado do Piauí [Epidemiology and symptoms of conidiobolomycosis in sheep in the State of Piauí, Brazil]. *Pesq Vet Bras*. 2007b;27(4):184-190.
24. Shaikh N, Hussain KA, Petraitiene R, Schuetz AN, Walsh TJ. Entomophthoramycosis: a neglected tropical mycosis. *Clin Microbiol Infect*. 2016;22(8):688-94.
25. Tabosa IM, Riet-Correa F, Nobre VMT, Azevedo EO, Reis-Junior JL, Medeiros RM. Outbreaks of pythiosis in two flocks of sheep in northeastern Brazil. *Vet Pathol*. 2004;41:412-415.
26. Teifke JP, Klopfleisch R, Czerwinski G, et al. Morphologische, immunhistologische und molekulare Untersuchungen zur Pathogenese der enzootischen Nasentumoren beim Schaf. *Tierärztl Prax*. 2007;35:264-272.
27. Ubiali DG, Cruz RAS, de Paula DAJ, et al. Pathology of nasal infection caused by *Conidioboulus lamprauges* and *Pythium insidiosum* in sheep. *J Comp Pathol*. 2013;149:137-145.
28. Vilela R, Mendoza L. Human Pathogenic Entomophthorales. *Clin Microbiol Rev.* 2018 ;31(4):e00014-18.
29. Vilela R, Silva SMS, Riet-Correa F, Dominguez E, Mendoza L. Morphologic and phylogenetic characterization of *Conidiobolus lamprauges* recovered from infected sheep. *J Clin Microbiol*. 2010;48(2): 427-432.

CASE IV:

Signalment:
5 year old castrated male Nubian goat (*Capra aegagrus hircus*).

History:
The goat presented to Ohio State Large Animal Services with a 10-day history of lethargy, depression and difficulty standing. Previously he had a wet cough that resolved with Nuflor by the rDVM, though he continued to have mucopurulent discharge and a mild cough. Upon presentation, he was quiet, alert, responsive, and in sternal recumbency. Bloodwork suggested renal disease based on azotemia and metabolic acidosis (see laboratory results below), with an unremarkable urinary bladder and small hypoechoic region in the renal medulla on ultrasound. He received a blood transfusion and fluid therapy, but was not observed to urinate. He continued to decline clinically, and was humanely euthanized.

Gross Pathology:

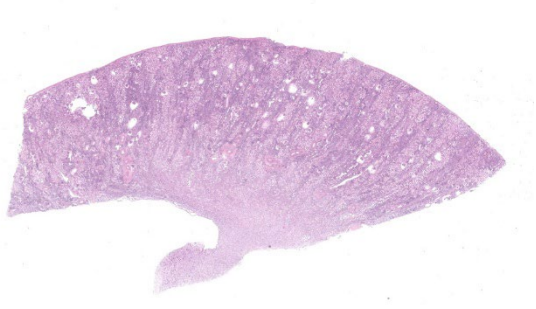

Figure 4-1: Kidney, goat. A single section of kidney is submitted for examination. (HE, 10X)

On gross examination, there was mild serosanguineous pericardial effusion, similar fluid within the entire length of the trachea as well as pulmonary edema. The urogenital tract was unremarkable.

Laboratory Results:

PCV/TP:

- Pre-transfusion = 11/ 7.4
- Post-transfusion = 17/ 6.4

NOVA Panel:

- pH = 7.467
- BUN = 303mg/dL
- Creatinine = 15.5mg/dL
- pCO_2 = 31.4mmHg
- HCO_3 = 22.9mmol/L

Biochemistry Profile:

- BUN = 380mg/dL
- Creatinine = 17.8mg/dL
- Phosphorous = 4.5mg/dL
- Calcium (total) = 7.7mg/dL
- Sodium = 138meq/dL
- Potassium = 3.73meq/dL
- Chloride = 86.7meq/dL
- Anion Gap = 39meq/dL
- Total protein = 5.8g/dL
- Albumin = 3.1g/dL
- Globulin = 2.7g/dL

Hemogram/ CBC:

- Plasma protein = 7.8g/dL
- HCT = 15%
- Hemoglobin = 3.8g/dL
- RBC = 7.3x10^12/L
- MCHC = 25.7g/dL
- Retic absolute = 32.1x10^9/L
- Total leukocytes = 19.9x10^9/L
- Seg neutrophils = 16.9x10^9/L
- Lymphocytes = 3.0x10^9/L

Parasitology (McMaster's Fecal Float):

- Few strongyles and occasional Eimeria were detected in post-mortem colonic contents. No parasites were detectable in the posts-mortem abomasal contents.

Microscopic Description:

There are multiple sections of kidney that include cortex, medulla, and papilla. All of the glomeruli are affected to varying degrees of severity. The glomeruli are globally hypercellular, within both the endocapillary and mesangial compartments. Capillary walls are markedly thickened by eosinophilic matrix. There is frequent dilation of Bowman's capsules and segmental collapsed glomerular tufts/ capillaries with expansion of mesangium with eosinophilic matrix (segmental sclerosis). Less than 25% of the glomeruli are globally sclerotic. Occasionally glomerular tufts are segmentally to globally effaced by eosinophilic mesangial matrix, and mesangial and intracapillary dark brown (hemosiderin) and yellow (hematoidin) pigment with scattered hemosiderin laden macrophages within Bowman's space. There is infrequent segmental loss of podocytes with proliferation of eosinophilic matrix and cells that adhere the glomerular tuft to Bowman's capsule (crescents). Several glomerular capillary loops are filled with fibrin thrombi.

Over half of the tubules are characterized by attenuated epithelium, sloughed hypereosinophilic necrotic intraluminal epithelium, and/or piling of basophilic tubular ep

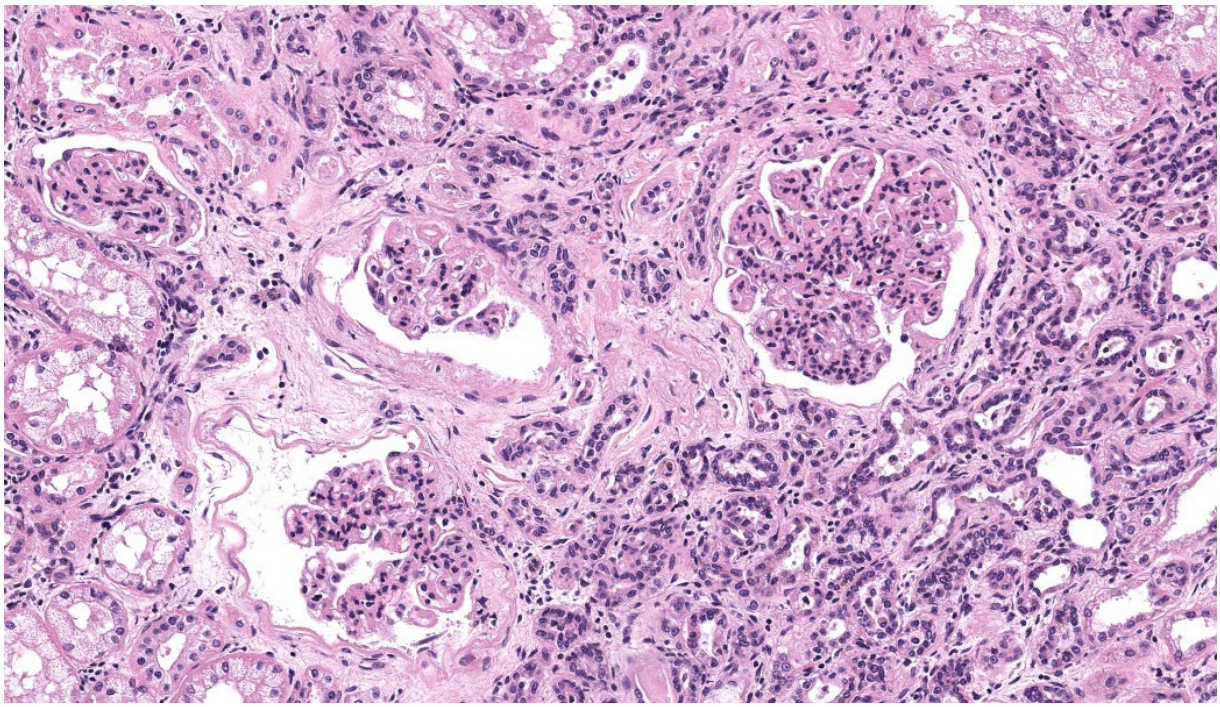

Figure 4-2: Kidney, goat. Glomeruli demonstrate global enlargement, mesangial hypercellularity, expansion of capillary loops, thickening of Bowman's capsule and periglomerular fibrosis. The interstitium is expanded by fibrous connective tissue with entrapped and atrophic tubules. (HE, 381X)

ithelium (regeneration). Often tubules are dilated with eosinophilic proteinaceous material (hyaline casts), and contain intraluminal basophilic refractile material (mineralization). Infrequently, tubules are filled with degenerate neutrophils. There is a mild loss of tubules with expansion of the interstitium by fibrous matrix and aggregates of lymphocytes with fewer plasma cells. There are multiple arcuate arteries with an expanded tunica intima by increased numbers of smooth muscle cells and fibrous matrix, and/or thickened and hypercellular tunica medias (arteriosclerosis).

Special stains included Masson's trichrome, periodicacid-Schiff (PAS), and Jones methenamine silver (JMS). The PAS demonstrated that the thickened mesangium and glomerular capillary loops were expanded by PAS positive material that often-formed double contours, spike-like projections and encircled bright magenta deposits using the Trichrome stain. Both the PAS and trichrome highlight the collapsed capillary loops of the globally sclerotic glomeruli with expansion of Trichrome and PAS-positive matrix.

Three glomeruli were available for ultrastructural evaluation by transmission electron microscopy (TEM). One glomerulus had collapsed capillary loops and fibrillary material in Bowman's space. All glomeruli had numerous large electron dense deposits within the capillary walls in intramembranous, subendothelial, mesangial, and subepithelial locations. Subepithelial deposits were associated with spike-like projections and circulations of glomerular basement membrane material. One glomerulus is segmentally sclerotic with loss of podocytes and denuded capillary walls. The afferent/ efferent arterioles have severely hypertrophied endothelial cells with markedly narrow lumens. In one of the arterioles the circulating erythrocytes are distorted.

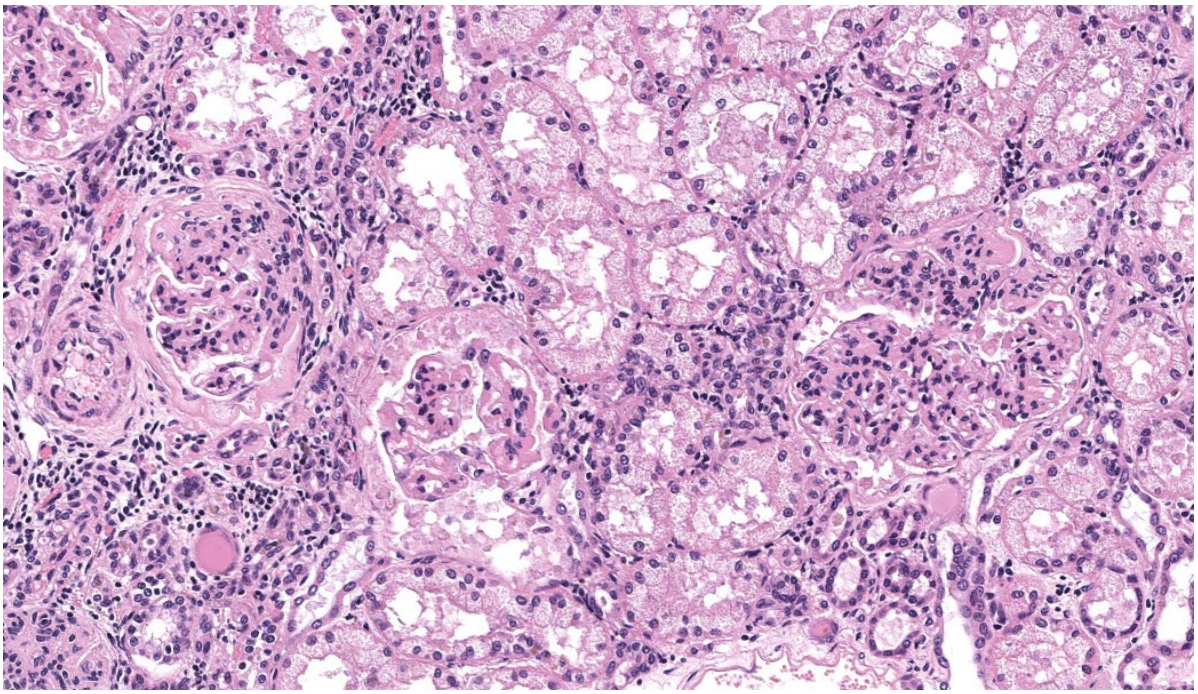

Figure 4-3: Kidney, goat. In this field, glomeruli demonstrate segmental sclerosis as well as synechia formation (glomerulus), mesangial hypercellularity, expansion of capillary loops, thickening of Bowman's capsule and periglomerular fibrosis. Tubular epithelium is degenerative with cell swelling and vacuolation, and there are numerous individualized and aggregated lymphocytes and plasma cells. The interstitial is expanded by fibrous connective tissue with entrapped and atrophic tubules. (HE, 381X)

Contributor's Morphologic Diagnoses:
Kidney: Diffuse global to segmental marked chronic active immune complex mediated membranoproliferative glomerulonephritis with superimposed thrombotic microangiopathy, tubular necrosis and atrophy, interstitial fibrosis and lymphoplasmacytic interstitial nephritis

Contributor's Comment:
Immune complex (IC) glomerulonephritis (GN) is classified as membranous, proliferative, mesangioproliferative, and membranoproliferative. Membranous glomerulonephritis is characterized by a remodeled basement membrane secondary to IC deposition on the abluminal surface of the glomerular basement membrane leading to normocellularity to mild hypercellularity. Proliferative glomerulonephritis histologically has increased cellularity without alterations to the glomerular basement membranes and may be associated with IC deposition. Histologically, mesangioproliferative glomerulonephritis has increased cellularity within the mesangium with IC deposition usually between the endothelium and the glomerular basement membrane. Membranoproliferative glomerulonephritis (MPGN) is characterized by endocapillary and mesangial cell proliferation with remodeling of the capillary loop due to IC deposition usually between the endothelium and the glomerular basement membrane[4]. In the present case, the immune complexes were present in multiple locations hence the use of "mixed MPGN".

ICGN results from circulating antigen-antibody complexes of non-glomerular origin

that localize in the glomerulus and are able to be detected via immunofluorescence or TEM

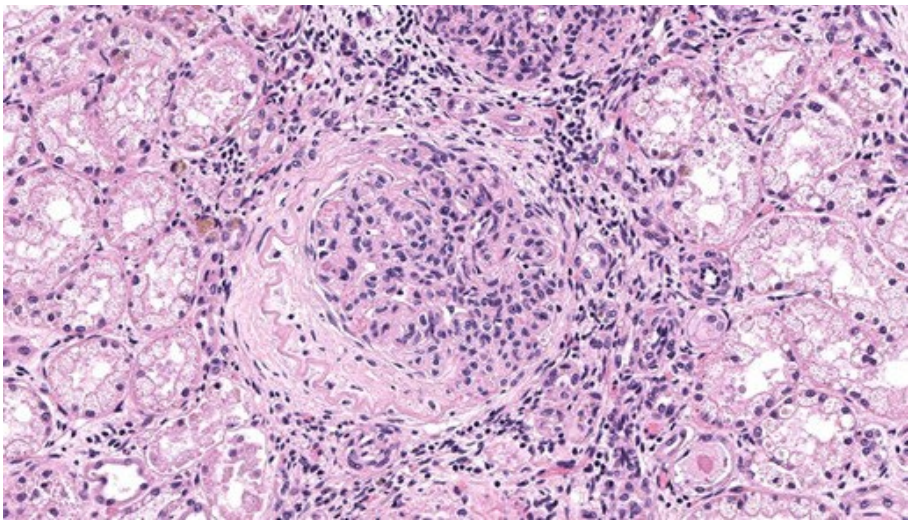

Figure 4-4: Kidney, goat. A hypercellular glomerulus with marked expansion of capillary loops and synechiae formation. (HE, 576X)

as electron-dense deposits. The immune complexes often contain complement, as well. IC deposition is thought to occur when concentrations of antigen and antibody are equal, or when antigens are in slight excess in comparison to antibody concentrations.[4] Another hypothesis is that some antigens, such as those derived from viruses like feline leukemia virus, bacteria, and parasites, such as *Dirofilaria,* can lead to immune complex deposi tion.[4,2] Experimentally, chronic antigenemia leading to ICGN is modeled by repeatedly injecting small doses of endogenous or exogenous antigens. Although caprine arthritis and encephalitis virus (CAEV) has not been previously reported to cause ICGN in goats, the herd of the present case was positive for CAEV and is thought to be the source of consistent antigen stimulation. There was a study on naturally infected sheep with Maedi-visna virus and associated glomerular lesions; however, there was lack of TEM and glomerular staining (PAS, JMS, and Trichrome) to fully characterize the lesions of ICGN.[1]

Thrombotic microangiopathy is characterized by endothelial cell damage that potentially produces thrombocytopenia and hyaline thrombi.[3,6] Causes include genetic factors, malignant hypertension, pregnancy, drugs, transplantation, and infections.[3] TMA is the lesion in greyhounds with idiopathic cutaneous and renal glomerular vasculopathy, as well as the well-characterized hemolytic uremic syndrome in humans associated with shiga or shiga-like exotoxin of *Escherichia coli* O157:H7.[3,4] In humans there are also several viruses associated with and thought to cause TMA.[3,6] Therefore, in the present case, the superimposed lesion of TMA is likely related to CAEV infection and/or hypertension. The acute tubular necrosis in this case is likely

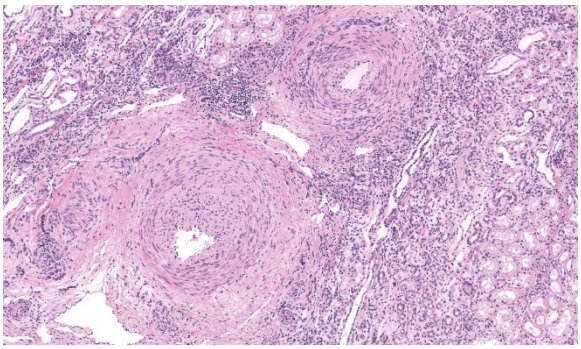

Figure 4-5: Kidney, goat. There is asymmetric mural hyperplasia and tortuosity of arcuate arterioles. There is loss of the inner elastic lamina for mural proliferation of smooth muscle cells and fibroblasts, and circumferential lamellations of collagen and fibroblasts within the adventitia. (HE, 400X).

related to ischemia possibly related to the vasculopathy as indicated by the arcuate arteriosclerosis and TMA lesions.

Contributing Institution:
The Ohio State University, Department of Veterinary Biosciences, Columbus Oh. www.vet.osu.edu

JPC Diagnoses:
Kidney: Glomerulonephritis, membranoproliferative, chronic, diffuse, severe, with glomerulosclerosis, lymphoplasmacytic interstitial nephritis, tubular degeneration, necrosis, and regeneration, and arteriolar fibrointimal hyperplasia and sclerosis.

JPC Comment:
Closing out our fourth conference, this case graced participants with an opportunity to see a lovely correlation between light microscopy and electron microscopy (EM) findings. It's not often that EM images are sent in as part of Wednesday Slide Conference submissions, but it's always a treat when they are! Many thanks to the contributor for providing both a wonderful slide and beautiful EM images. Together, they truly did paint the whole picture for this EM-worthy condition.

Because the EM images were provided, a review of the ultrastructural anatomy of a glomerular capillary profile and its surrounding structures ensued, with focus on the primary and secondary foot processes of the visible podocyte and the different layers of the glomerulus. However, the main show was the electron-dense, granular, irregularly shaped clumps of immune complexes (IC) within subepithelial, intramembranous, and subendothelial spaces of the glomerular tuft. Having IC deposition demonstrably in all three of those locations within the glomerulus assisted with the determination of the "mixed" type of glomerulonephritis in this case. Conference participants favored "membranoproliferative" based on the H&E slide, but acknowledged that this case did not fit 100% into that box upon review of the EM images and accepted the use of the term "mixed" in discussion. Typing of glomerulonephritis is more difficult to do with light microscopy alone due to some histologic similarities between the types, bringing home the point that, for definitive characterization of glomerulonephritis, EM is indispensable.

There was discourse on differentiating membranoproliferative from membranous glomerulonephritis based on histologic features, as some conference participants went one way or the other in their morphologic diagnoses. To summarize, membranoproliferative glomerulonephritis will have an increased number of nuclei within the glomerular tuft, mesangial cell proliferation, and often, the presence of recruited neutrophils. Membranous glomerulonephritis typically just has an increased amount (thickening) of basement membranes with little cellular proliferation within the glomerular tuft. One conference participant inquired on the histologic differences between synechiae and crescents in the glomerulus. Synechiae were described as the touching of the visceral layer of Bowman's capsule to the parietal layer without fibrosis, whereas crescents have a fibrous component and demonstrate full adhesion of the glomerulus to the capsule. Conference participants did not think there was enough histologic evidence of thrombotic microangiopathy include it in the morphologic diagnosis in this particular case.

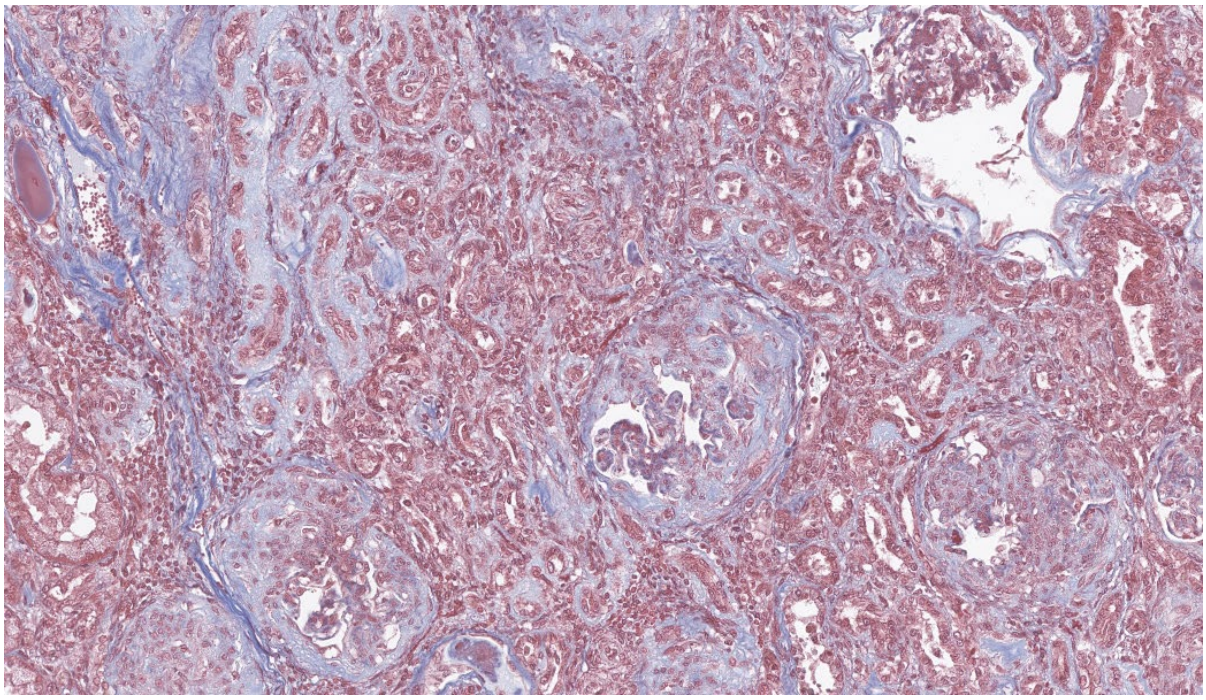

Figure 4-6: Kidney, goat. A Masson's stain demonstrates the amount of collagen within the glomerular mesangium associated with segmental sclerosis, the periglomerular fibrosis, and the interstitial expansion by collagen. (Masson's trichrome, 545X)

So, the renal glomerulus…what a champion. The glomerulus is a physiologic heavy lifter made up of three distinct layers: fenestrated endothelium, basement membrane, and podocytes. These layers enable the glomerulus to fulfill its destiny as a highly selective filter of blood based on compound size and charge, ridding the body of wastes while retaining essential materials. Glomerular filtrate is passed into the surrounding Bowman's capsule before moving into the proximal convoluted tubules to continue its journey. For all its hard work and contributions to the bodily society, glomeruli are relatively fragile and prone to injury. Immune-complex glomerulonephritis occurs when the concentration of antigen-antibody complexes within the body becomes too high for the body to clear in a timely fashion. The size, charge, and insolubility of ICs, along with excessive complement activation secondary to their deposition, can overwhelm the body's clearance mechanisms and result in deposition into the glomerulus.

Complexes are deposited into glomerular capillaries due to the basement membrane's negative charge. The basement membrane will attract positively charged pre-formed complexes, but can also form IC complexes on itself if a positively charged antigen binds to the glomerulus directly and is then tagged by an antibody.[5] The ICs trigger an immune response by either calling in inflammatory cells via their sheer presence or by activating resident glomerular cells to release cytokines, vasoactive substances, and prothrombotic compounds. Either way, this ultimately damages the endothelium, epithelium, and mesangium of the affected glomerulus, resulting in glomerulonephritis.[5]

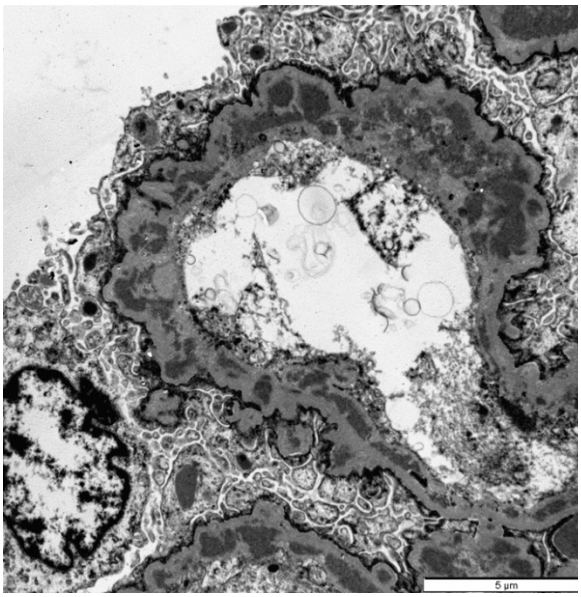

Figure 4-7: Kidney, goat. All glomeruli had numerous large electron dense deposits within the capillary walls in intramembranous, subendothelial, mesangial, and subepithelial locations. Subepithelial deposits were associated with spike-like projections and circulations of glomerular basement membrane material. (Photo courtesy of: The Ohio State University, Department of Veterinary Biosciences, Columbus Oh. www.vet.osu.edu)

The primary mediator of IC glomerulonephritis is the complement system, specifically the membrane attack complex (MAC), which is made up of complement components C5b complexed with C6-9 to create C5b6789. The MAC generally does not achieve sufficient quantities to result in cell lysis in this IC glomerulonephritis, but inserts into the membranes of glomerular cells and causes their conversion into resident inflammatory effector cells that then damage the glomerulus.[5]

Couple this process with the lymphocytes and plasma cells that show up in response, the poor affected glomerulus is set on a course of irreversible damage. Mesangial cells and capillary endothelial cells try their best to combat the glomerular destruction by proliferating and remodeling, hence the "proliferative" part of this diagnosis, but this can only do so much if the antigen-antibody complexes continue to circulate in high numbers and continuously deposit into glomeruli.

All in all, this case was easily the most heavily discussed both during conference and the morphologic diagnosis session, where there was highly spirited discussion between staff on the most appropriate morphologic diagnosis. The attending residents were able to hear a variety of opinions on these lesions and, ultimately, consensus (more or less) was reached. Many thanks again to this contributor for a truly high-value learning case!

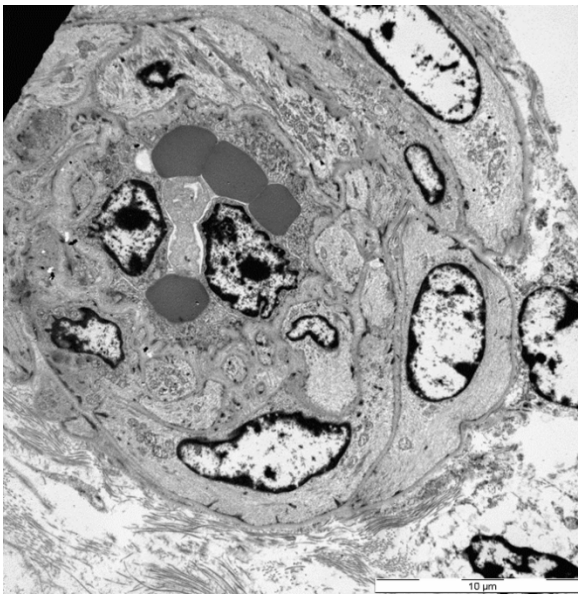

Figure 4-8: Kidney, goat. In sclerotic glomeruli, the afferent/ efferent arterioles have severely hypertrophied endothelial cells with markedly narrow lumens. (Photo courtesy of: The Ohio State University, Department of Veterinary Biosciences, Columbus Oh. www.vet.osu.edu)

References:

1. Angelopoulou K, Brellou GD, Vlemmas I. Detection of maedi-visna virus in the kidneys of naturally infected sheep. *Journal of comparative pathology*. 2006;134: 329-335.
2. Long JD, Rutledge SM, Sise ME. Autoimmune Kidney Diseases Associated with Chronic Viral Infections. *Rheumatic diseases clinics of North America*. 2018;44: 675-698.
3. Lopes da Silva R. Viral-associated thrombotic microangiopathies. *Hematology/oncology and stem cell therapy*. 2011;4: 51-59.
4. Maxie MG. *Jubb, Kennedy, and Palmer's pathology of domestic animals*, Sixth ed., vol. 2. St. Louis (MO): Elsevier; 2016.
5. Nangaku M, Couser WG. Mechanisms of immune-deposit formation and the mediation of immune renal injury. *Clin Exp Nephrol*. 2005;9(3):183-91.
6. Salter T, Burton H, Douthwaite S, Newsholme W, Horsfield C, Hilton R. Immune Complex Mediated Glomerulonephritis with Acute Thrombotic Microangiopathy following Newly Detected Hepatitis B Virus Infection in a Kidney Transplant Recipient. *Case reports in transplantation*. 2016;2016**:** 3152495.
7. Sementilli A, Moura LA, Franco MF. The role of electron microscopy for the diagnosis of glomerulopathies. *Sao Paulo Med J.* 2004;122(3):104-9.